International Journal of Minerals, Metallurgy and Materials
Volume 23, Number 1, January 2016, Page 109
DOI: 10.1007/s12613-016-1217-0

Synthesis of crystalline perovskite-structured $SrTiO_3$ nanoparticles using an alkali hydrothermal process

U.K.N. Din, T.H.T. Aziz, M.M. Salleh, and A.A. Umar

Institute of Microengineering and Nanoelectronics (IMEN), Universiti Kebangsaan Malaysia, Bangi 43600, Selangor, Malaysia

(Received: 19 June 2015; revised: 13 August 2015; accepted 1 September 2015)

Abstract: We report an experimental route for synthesizing perovskite-structured strontium titanate ($SrTiO_3$) nanocubes using an alkali hydrothermal process at low temperatures without further heating. Furthermore, we studied the influence of heating time (at 180°C) on the crystallinity, morphology, and perovskite phase formation of $SrTiO_3$. The $SrTiO_3$ powder, which is formed via nanocube agglomeration, transforms into cubic particles with a particle size of 120–150 nm after 6 h of hydrothermal sintering. The crystallinity and percentage of the perovskite phase in the product increased with heating time. The cubic particles contained 31.24at% anatase TiO_2 that originated from the precursor. By varying the weight ratio of anatase TiO_2 used to react with the strontium salt precursor, we reduced the anatase-TiO_2 content to 18.8at%. However, the average particle size increased when the anatase-TiO_2 content decreased.

Keywords: strontium titanate; nanoparticles; anatase; hydrothermal synthesis

1. Introduction

Perovskite-type compounds have attracted widespread interest because of their technological importance in optoelectronic devices, such as in solar cells as organometal halide perovskites [1] and in host fluorescence materials as fluoride perovskites [2]. However, perovskite-type oxides are particularly interesting because of their functional properties, including their nonlinear optical coefficients and dielectric constants [3]. Strontium titanate ($SrTiO_3$) is a member of the perovskite-type oxide family with an ABO_3 chemical formula; it displays a cubic structure. $SrTiO_3$ is typically synthesized using a solid-state approach that does not influence the physical characteristics of the resulting perovskite. The primary factor that controls the $SrTiO_3$ phase and morphology to result in a compound with desirable properties is the fabrication route, precursors, and preparation method [4]. To achieve nanostructural physical control of $SrTiO_3$, researchers have developed several methods that involve different raw materials and restricted conditions to vary the perovskite phase, morphology, particle size, and crystal defects [5].

The conventional synthesis route requires high temperatures and long calcination times. The typical polymeric complex method for synthesizing $SrTiO_3$ involves high temperatures in the range from 600 to 1200°C and calcination for approximately 10 h [6]. The heating time is reduced to 2 h in the case of the sol–gel combustion method [7] and 10 h for the liquid–solid reaction method [8]; in addition, $SrTiO_3$ is synthesized in the temperature range from 500 to 800°C in these methods. Moreover, several techniques, such as the solvothermal [9] and sol–gel hydrothermal approaches [10], are available for synthesizing $SrTiO_3$ at lower temperatures between 180 and 260°C; however, a longer heating time (18–48 h) is required. When using these methods, the lack of nanostructural phase control to prepare perovskites optimized for practical applications will likely become a constraint. In the absence of a physical control process, the perovskite nanostructure will exhibit poor optical properties [11].

Several lower-temperature methods with shorter heating times have been developed for synthesizing $SrTiO_3$, such as a hydrothermal method [12] and a wet chemical method that involves hydrolysis and a hydrated titania gel [13]. None-

Corresponding author: U.K.N. Din, E-mail: ummiump@yahoo.com; M.M. Salleh, E-mail:mms@ukm.edu.my

theless, the anatase-TiO_2 and $SrCO_3$ residues in the $SrTiO_3$ products affect the perovskite phase formation. Among the aforementioned $SrTiO_3$ synthesis methods, the alkali hydrothermal process is an excellent choice for obtaining $SrTiO_3$ with good optical properties because of the ability to control the morphology and shape through chemical purity and homogeneity [14]. This approach provides a highly crystalline product with good phase purity. The alkali hydrothermal process, which uses a strontium salt and anatase TiO_2 as raw materials, produces a perovskite with high phase purity using a relatively low temperature and a short reaction time [15]. This process is facile, cost-effective, and time efficient. Furthermore, high-quality, crystalline $SrTiO_3$ can be obtained at a lower temperature and without unwanted residues in the structure by varying the anatase TiO_2 weight ratio in the precursor.

Inspired by these considerations, we here focus on the synthesis and characterization of cubic perovskite $SrTiO_3$ using anatase TiO_2 and strontium salt precursors via the alkali hydrothermal process. The material characterization was performed using X-ray diffraction (XRD) and field-emission scanning electron microscopy (FESEM). Our aim was to study the influence of the alkali hydrothermal process reaction time and the anatase TiO_2 weight ratio on the crystallinity, morphology, and the percentage of $SrTiO_3$ perovskite in the product. This work represents the first investigation of the influence of these properties through variation of the composition of the anatase TiO_2 and strontium salt precursor at low temperatures to produce a highly crystalline perovskite oxide, $SrTiO_3$. Because it provides control of the particle size and certain morphological features, this method will be useful in the preparation of perovskite-structured electronic materials with novel applications.

2. Experimental

2.1. Materials

Strontium chloride hexahydrate ($SrCl_2·6H_2O$) (ACS reagent, 99%, Sigma-Aldrich, Japan), and titanium(IV) oxide (TiO_2, anatase powder, 99.8%, Aldrich Chemistry, Canada) were used as the raw materials. Sodium hydroxide (NaOH) pellets (Macron, Sweden) were used as a mineralizer. Acetic acid (CH_3COOH) (ACS reagent, 99.7%, (Sigma-Aldrich, Germany) and absolute ethanol (R&M, France) were used as solvents in the reaction and to subsequently wash the precipitate. For the hydrothermal process, deionized water was used for the aqueous solutions. The chemicals used for these experiments were analytical-grade reagents and were used without further treatment.

2.2. Synthesis of cubic $SrTiO_3$ powder

The $SrTiO_3$ perovskite powder was synthesized using the alkali hydrothermal method. Specifically, 0.5 g of anatase TiO_2 and 1.7 g of $SrCl_2·6H_2O$ were dissolved in 50 mL of deionized water under continuous stirring for 15 min at 700 r/min. The mixture was then bubbled with nitrogen (N_2) gas for approximately 8 min to eliminate dissolved carbon dioxide. To mineralize and thereby stabilize the solution, 2 g of NaOH (1 M) was subsequently added to the aqueous solution. After the mixture was stirred for approximately 8 min at room temperature, a milky sol was obtained. The as-prepared sol was transferred to a Teflon-lined stainless steel autoclave with a filling volume of 8 mL (90% of the total volume). The hydrothermal treatment was performed at different heating times (from 1 to 10 h) at 180°C to investigate the effect of the heating time on the optical properties of the resulting $SrTiO_3$ perovskite. The autoclave was allowed to naturally cool to ambient temperature. The resulting material was filtered and thoroughly washed with absolute ethanol and acetic acid. The filtered sample was dried for 14 h at 50°C in a drying oven. Finally, $SrTiO_3$ powders were obtained. Further experiments were performed in which the weight ratio of anatase TiO_2 (from 20wt% to 60wt% of the initial concentration of anatase TiO_2) and the heating time (from 6 to 8 h) were varied.

2.3. $SrTiO_3$ powder characterization

The crystallinity of the structure and the phase purity of $SrTiO_3$ were characterized using X-ray diffraction (XRD) measurements. The XRD patterns of the perovskite powder were collected using a Philips X'Pert Materials Research diffractometer equipped with a Cu-K_α monochromatic radiation source (λ = 0.1541 nm) operated at 40 kV and 30 mA. The parameters for all XRD scans were a scan speed of 2.0°/min, a step size of 0.016°, and a scanned 2θ range of 5° to 80°. The $SrTiO_3$ powder crystallite sizes were calculated using X-ray line broadening analysis according to the Scherrer equation [16]. The relative amounts of perovskite and residue phases were determined on the basis of the intensity of the 110 reflection of the perovskite phase (I_p) and that of the 101 reflection of the residue phase (I_m) using the aforementioned equation [17]. The morphology and size of the prepared $SrTiO_3$ nanoparticles were observed using a field-emission scanning electron microscope (LEO SUPRA 55VP) operated at an accelerating voltage of 20 kV.

3. Results and discussion

3.1. Influence of alkali hydrothermal reaction time on the crystallinity, morphology, and the percentage of the perovskite phase

The XRD patterns of the as-prepared $SrTiO_3$ powder samples, which were synthesized at 180°C and at different heating times ranging from 1 to 10 h, are shown in Fig. 1. The XRD pattern revealed peaks corresponding to the (100), (110), (111), (200), (210), (211), (220), (300), and (310) planes of $SrTiO_3$. In the case of the $SrTiO_3$ sample reacted for 1 h, all of the diffraction peaks were indexed to cubic $SrTiO_3$ and matched the peaks in the standard pattern; the lattice constant of the prepared $SrTiO_3$ was a = 0.39050 nm. All of these peaks correspond to the cubic structure of $SrTiO_3$ according to Joint Committee on Powder Diffraction Standards (JCPDS) card No. 35-0734. Fig. 1(a) shows the XRD pattern of the $SrTiO_3$ sample reacted for 1 h; it exhibits a high-intensity peak at 25.3° with *hkl* indices of 101. This peak indicates the presence of anatase TiO_2, which originates from the second precursor solution during synthesis. Additionally, the tetragonal structure of anatase TiO_2 with a lattice constant of a = 0.37852 nm and c = 0.95083 nm, matches the standard pattern (JCPDS No. 21-1272).

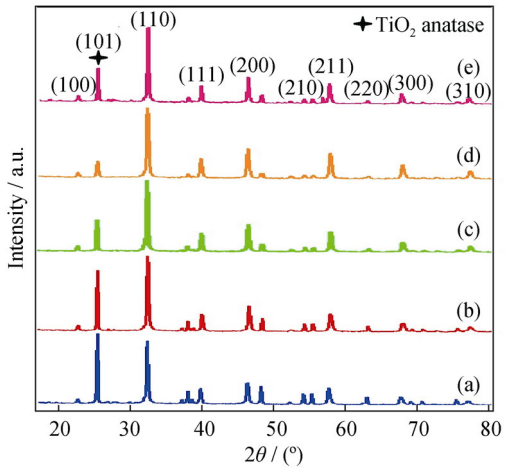

Fig. 1. X-ray diffraction patterns of $SrTiO_3$ synthesized at 180°C using different heating times: (a) 1 h; (b) 3 h; (c) 6 h; (d) 8 h; (e) 10 h.

The predominance of anatase-TiO_2 residue in the formed perovskite phase is clearly evident in the XRD pattern, and $SrTiO_3$ is poorly crystallized after 1 h of reaction time. Furthermore, after 3 h of reaction, the perovskite phase exhibited substantially improved crystallinity, even though the presence of a minor anatase-TiO_2 residue phase was evident in the XRD pattern. This result indicates that a well-crystallized $SrTiO_3$ product was obtained with a short reaction time of 3 h. A short reaction time is required because a simple chemical reaction occurs between the strontium salt and the anatase-TiO_2 precursor via the hydrothermal process. Although the anatase-TiO_2 residue phase was formed, its concentration was reduced. With an increase in the reaction time, the diffraction peaks of the $SrTiO_3$ perovskite became more intense and sharper, thereby demonstrating that the degree of crystallization of the products improved and that the product quality increased as the reaction time was extended.

The average crystallite size (D) of $SrTiO_3$ was calculated using the Scherrer equation, $D = \frac{K\lambda}{\beta \cos\theta}$, where D is the grain size, K = 0.9 and is a correction factor, β is the full-width at half- maximum (FWHM) of the most intense diffraction peak (in this study, the (110) plane), λ is the X-ray wavelength (Cu-K_α radiation, λ = 0.0154056 nm), and θ is the Bragg angle [16]. The FWHM values decreased with decreasing heating time. With an increase in the heating time, the crystallization and grain size increased, resulting in a decrease in the FWHM values. We expected the grains to coalesce when the heating time was increased and that this coalescence would result in a larger grain size [15]. The increase in diffraction peak intensity and crystallization depends on the increase in heating time, as was confirmed by an enhancement in the crystallinity of the perovskite powder.

The percentage of perovskite-phase $SrTiO_3$ powder in the product increased with increasing heating time (Table 1). However, after 10 h of heating, the intensities of the $SrTiO_3$ peaks decreased. This decreased intensity is attributed to degradation of the crystallites upon prolonged heating [18]. Thus, the perovskite-phase component of the reaction products decreased by at 3.66at%. For 6 h of reaction time, the cubic particles contained 31.24at% of anatase TiO_2, indicating 68.76at% of perovskite-phase $SrTiO_3$. The optimal value for sintering $SrTiO_3$ perovskite was defined by the influence of the perovskite phase after 8 h of reaction time.

The FESEM images of perovskite nanoparticles ($SrTiO_3$) in Fig. 2 show the surface morphologies of the cubic structures synthesized at different heating times from 1 to 10 h. The as-prepared $SrTiO_3$ perovskite belongs to a centrosymmetric primitive cubic space group. During perovskite phase formation, the nanocubes coalesced and agglomerated to form well-crystallized nanoparticles with a low porosity. The morphologies of the time series of heated samples show the entire growth process for the $SrTiO_3$ cubic perovskite nanoparticles.

Throughout the phase formation, the nanoparticles exhibited a smooth surface and sharp edges. They were composed of TiO_2 nanoparticles, except in the cases of samples prepared using 1 and 3 h of sintering, where the morphologies

of the strontium salt and the anatase TiO_2 exhibited approximately cubic-spherical shapes and tetragonal shapes, respectively. However, in the case of the sample sintered 6 h, the spherically shaped particles gradually transformed into sharp-edged cubic particles. When the reaction time was further extended to 8 h, the sample morphologies retained their nanocubic structure, indicating that the perovskite $SrTiO_3$ particles were deficient in growth at 180°C, which is a substantially lower temperature than that reported for any previously produced perovskite [19–24]. As the heating time was increased, cubic-shaped particles were clearly observed to gradually form. However, after 10 h of reaction time, the cubic-shaped particles began to degrade because of the prolonged heating.

During 1–3 h of heating, the crystallite size increased by approximately 0.55 nm; it then substantially decreased from 3 to 6 h of heating. However, the grain size of the compound increased after 6–8 h of heating, which resulted in an average increase of 0.13 nm in the grain size, and remained unchanged after 10 h of heating. These observations are consistent with the XRD results, which indicated that the perovskite phase did not form when the sintering time was less than 3 h. These well-crystallized nanocubes presumably followed the crystallization growth process, which is consistent with the average crystallite size. The average $SrTiO_3$ particle size is shown in Table 1.

3.2. Influence of anatase-TiO_2 weight ratio on the crystallinity, morphology, and percentage of perovskite phase in the product

When the $SrTiO_3$ sintering time was less than 6 h, the average crystallite size and average particle diameter were inconsistent. This inconsistency is attributed to the fact that perovskite, when sintered for less than 6 h, is composed of

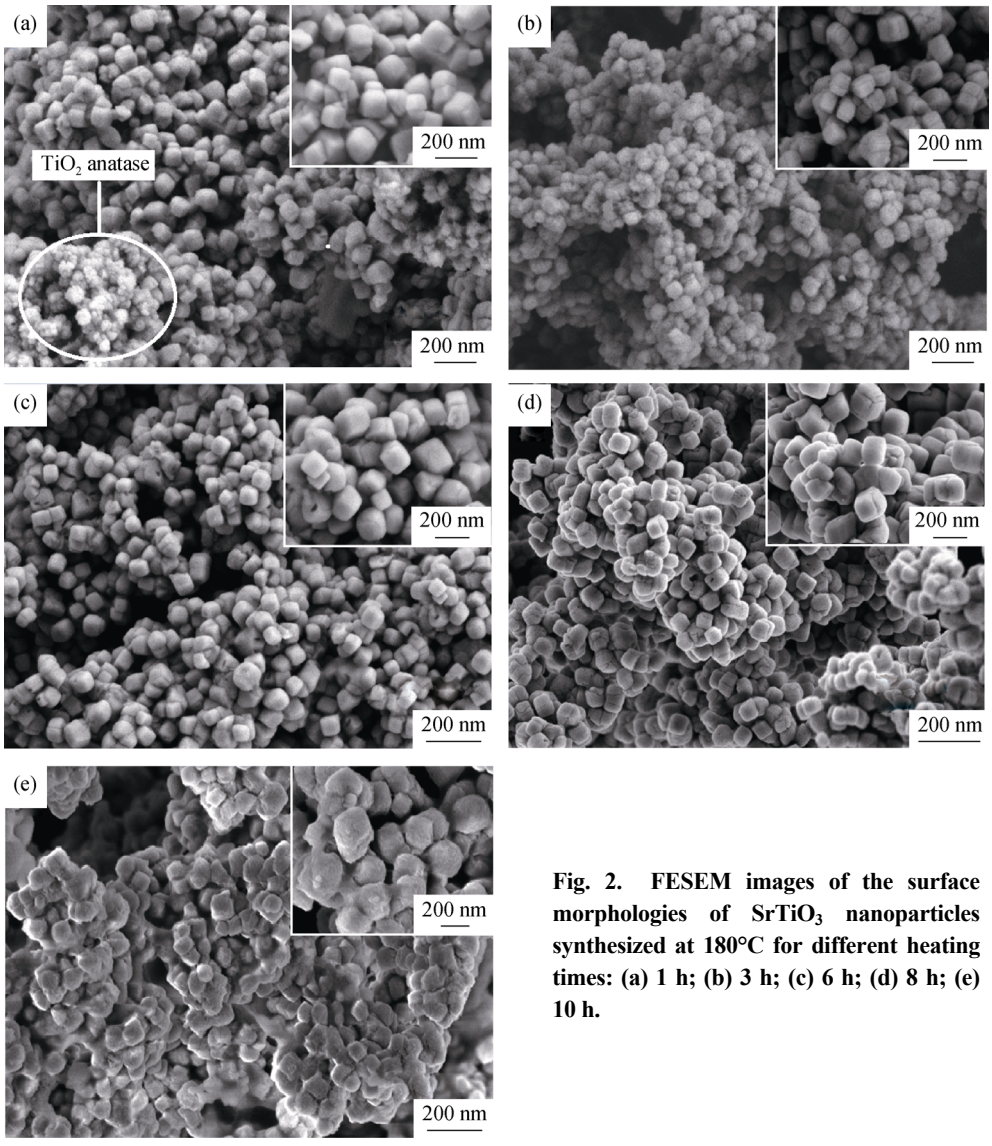

Fig. 2. FESEM images of the surface morphologies of $SrTiO_3$ nanoparticles synthesized at 180°C for different heating times: (a) 1 h; (b) 3 h; (c) 6 h; (d) 8 h; (e) 10 h.

Table 1. FWHM, average crystallite size, average particle size, and perovskite phase percentage of cubic $SrTiO_3$ as a function of heating time

Sintering time / h	FWHM / (°)	Average crystallite size / nm	Average particle size / nm	Perovskite phase / at%
1	0.44 ± 0.003	19.50	166.28	45.60
3	0.43 ± 0.001	20.05	120.22	54.80
6	0.44 ± 0.006	19.37	135.36	68.76
8	0.44 ± 0.003	19.50	150.40	70.30
10	0.44 ± 0.003	19.50	160.80	66.64

unreacted strontium salt and anatase TiO_2. These results suggest that the full phase transformation of perovskite is initiated after 6 h of sintering. Additionally, peaks attributable to anatase-TiO_2 residue were observed in the XRD pattern and the presence of this phase resulted in a lower perovskite phase percentage. Therefore, to improve the perovskite phase percentage, we performed an experiment in which the anatase-TiO_2 weight ratio was decreased in samples prepared using 6 and 8 h of sintering. The $SrTiO_3$ synthesis was conducted exactly as before, except the weight ratio of anatase TiO_2 was varied.

Fig. 3 shows the XRD patterns of the $SrTiO_3$ powders prepared using decreased percentages of anatase TiO_2 weight ratios (20wt%, 30wt%, 40wt%, and 60wt%) compared to the ratio used in the previous experiments. The XRD patterns of the as-prepared $SrTiO_3$ powders sintered at 180°C for 6 and 8 h indicated the formation of cubic $SrTiO_3$ with a minor residue of anatase TiO_2. Although the (101) peak of anatase TiO_2 was observed, the major peak of the perovskite increased in intensity and became sharper. Therefore, the crystallinity and percentage of the $SrTiO_3$ phase gradually increased after 6 h of sintering. Thus, we conclude that the percentage of the perovskite phase increased when a lower anatase-TiO_2 weight ratio was used. However, a significant decrease in the anatase-TiO_2 weight ratio resulted in some strontium salt precursor that did not react with TiO_2.

The FESEM images of the as-prepared perovskite nanoparticle ($SrTiO_3$) powders in Fig. 4 show the surface morphologies of the cubic-structured particles obtained after different heating times from 6 to 8 h. These images clearly reflect the decreased amounts of anatase TiO_2 (20wt%, 30wt%, 40wt% and 60wt%) compared to the amount used in the previous experiments. The perovskite $SrTiO_3$ was composed of cubic-like nanostructures whose shape and size were uniform among all of the samples. During the sintering process, after 6 and 8 h of heating, the crystallite size, which was determined using XRD, increased with each increase in the ratio of anatase TiO_2; the average increase was (0.3 ± 0.1) nm for each 20wt% of anatase TiO_2 added (Table 2).

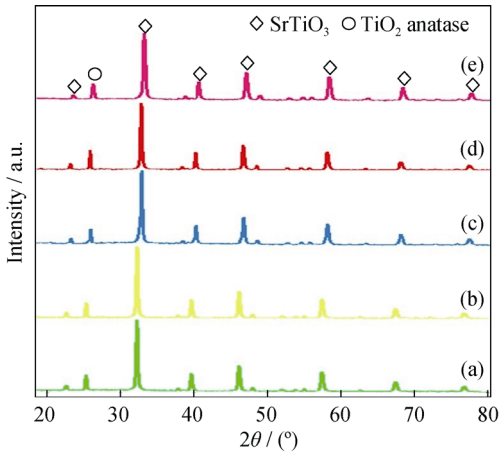

Fig. 3. XRD patterns of $SrTiO_3$ sintered at 180°C for different heating times in reactions where the amount of the TiO_2 precursor was decreased: (a) 6 h, 20wt% TiO_2; (b) 6 h, 30wt% TiO_2; (c) 6 h, 40wt% TiO_2; (d) 8 h, 40wt% TiO_2; (e) 8 h, 60wt% TiO_2.

Furthermore, whereas the crystallite size increased, the average particle size decreased with increasing weight ratio of anatase TiO_2. However, no pronounced change was observed in the surface morphology of the different samples. In this work, we did not obtain a pure $SrTiO_3$ phase because of the anatase-TiO_2 residue. During the synthesis process, the strontium salt and anatase-TiO_2 precursors may not have diffused well, which may have led to an imbalance in the solution homogeneity. Additionally, non-uniform heating could have occurred, resulting in the formation of an anatase-TiO_2 residue. The sample with the highest percentage of $SrTiO_3$ perovskite phase, which was defined as the sample with the highest crystallization with a preferential orientation at the (110) plane, was obtained after 6 h of heating with 30wt% anatase TiO_2, which resulted in 81.2at% perovskite phase, and 18.8at% remaining anatase TiO_2.

4. Conclusions

Perovskite $SrTiO_3$ nanoparticulate powders were synthesized at a low temperature of 180°C using the alkali hydrothermal process, without further heat treatment. The

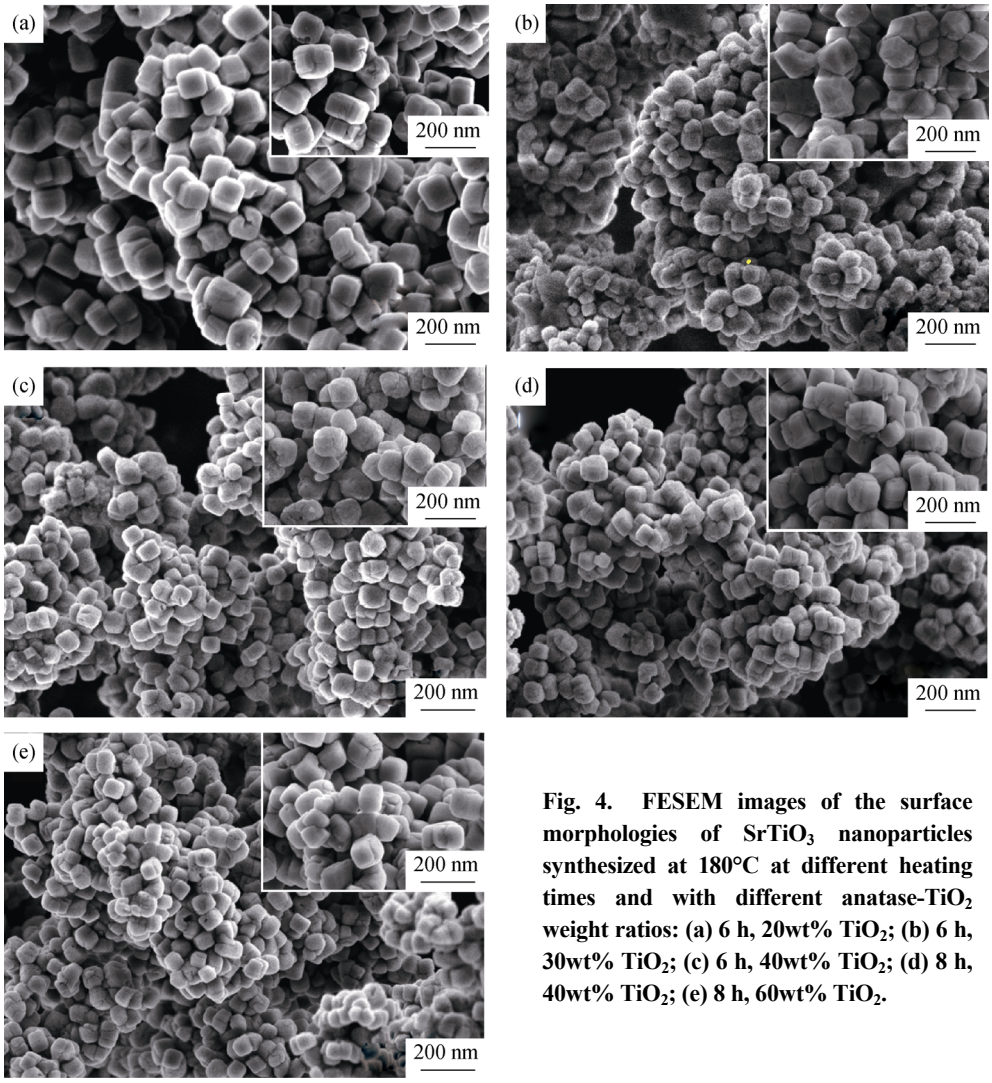

Fig. 4. FESEM images of the surface morphologies of $SrTiO_3$ nanoparticles synthesized at 180°C at different heating times and with different anatase-TiO_2 weight ratios: (a) 6 h, 20wt% TiO_2; (b) 6 h, 30wt% TiO_2; (c) 6 h, 40wt% TiO_2; (d) 8 h, 40wt% TiO_2; (e) 8 h, 60wt% TiO_2.

Table 2. Weight ratio of anatase TiO_2, FWHM, average crystallite size, average particle size, and percentage of cubic $SrTiO_3$ perovskite phase as a function of anatase-TiO_2 weight ratio

Sintering time / h	Weight ratio of TiO_2 anatase / wt%	Weight of TiO_2 anatase / g	FWHM / (°)	Average crystallite size / nm	Average particle size / nm	Perovskite phase / at%
6	20	0.10	0.45	19.20	155.28	79.10
6	30	0.15	0.44 ± 0.003	19.50	146.42	81.20
6	40	0.20	0.44 ± 0.003	19.50	138.60	79.33
8	40	0.20	0.44 ± 0.006	19.40	126.54	76.64
8	60	0.30	0.43 ± 0.006	19.80	121.12	77.67

experiments were conducted at different heating times and with different weight ratios of anatase TiO_2 used to react with a strontium salt. By controlling the heating time, we determined that 6 h of heating time was sufficient to obtain $SrTiO_3$ with high crystallinity and perfect morphological changes. Specifically, this reaction resulted in a transition from particles with cubic–spherical and tetragonal shapes to cubic particles with smooth surfaces, sharp edges, and a low porosity. When the anatase-TiO_2 weight ratio decreased, the amount of anatase TiO_2 in the $SrTiO_3$ perovskite product became minor. Thus, the $SrTiO_3$ nanoparticles exhibited a high crystallinity that resulted in a product containing 81.2at% perovskite phase.

Acknowledgements

The authors are grateful for the financial support from the Institute of Microengineering and Nanoelectronics, Univer-

siti Kebangsaan Malaysia under research grant (No. AP-2012-025).

References

[1] A. Kojima, K. Teshima, Y. Shirai, and T. Miyasaka, Organometal halide perovskites as visible-light sensitizers for photovoltaic cells, *J. Am. Chem. Soc*., 131(2009), No. 17, p. 6050.

[2] K. Yamada, K. Nakada, Y. Takeuchi, K. Nawa, and Y. Yamane, Tunable perovskite semiconductor $CH_3NH_3SnX_3$ (X: Cl, Br, or I) characterized by X-ray and DTA, *Bull. Chem. Soc. Jpn*., 84(2011), No. 9, p. 926.

[3] M.M. Saad, Strontium titanate perovskite $SrTiO_3$ as a promising ideal material for MEMS applications: first-principles FP-LMTO + LSDA Study, *J. Nat. Sci. Math*., 7(2014), No. 1, p. 1.

[4] S.C. Zhang, J.X. Liu, Y.X. Han, B.C. Chen, and X.G. Li, Formation mechanisms of $SrTiO_3$ nanoparticles under hydrothermal conditions, *Mater. Sci. Eng. B*, 110(2004), No. 1, p. 11.

[5] L.F. da Silva, W. Avansi, M.L. Moreira, A. Mesquita, L.J.Q. Maia, J. Andrés, E. Longo, and V.R. Mastelaro, Relationship between crystal shape, photoluminescence, and local structure in $SrTiO_3$ synthesized by microwave-assisted hydrothermal method, *J. Nanomater*., 2012(2012), p. 1.

[6] J.K. Park, H. Ryu, H.D. Park, and S.Y. Choi, Synthesis of $SrTiO_3$:Al,Pr phosphors from a complex precursor polymer and their luminescent properties, *J. Eur. Ceram. Soc*., 21(2001), No. 4, p. 535.

[7] T. Klaytae, P. Panthong, and S. Thountom, Preparation of nanocrystalline strontium titanate ($SrTiO_3$) powder by sol–gel combustion method, *Ceram. Int*., 39(2013), No. S1, p. S405.

[8] X.H. Liu and H.X. Bai, Liquid–solid reaction synthesis of $SrTiO_3$ submicron-sized particles, *Mater. Chem. Phys*., 127(2011), No. 1-2, p. 21.

[9] K. Nakashima, M. Kera, I. Fujii, and S. Wada, A new approach for the preparation of $SrTiO_3$ nanocubes, *Ceram. Int*., 39(2013), No. 3, p. 3231.

[10] S. Fuentes, R.A. Zarate, E. Chavez, P. Muñoz, D. Díaz-Droguett, and P. Leyton, Preparation of $SrTiO_3$ nanomaterial by a sol–gel-hydrothermal method, *J. Mater. Sci*., 45(2010), No. 6, p. 1448.

[11] S.F. Alvarado, F. La Mattina, and J.G. Bednorz, Electroluminescence in $SrTiO_3$:Cr single-crystal nonvolatile memory cells, *Appl. Phys. A*, 89(2007), No. 1, p. 85.

[12] W.J. Dong, X.Y. Li, J. Yu, W.C. Guo, B.J. Li, L. Tan, C.R. Li, J.J. Shi, and G. Wang, Porous $SrTiO_3$ spheres with enhanced photocatalytic performance, *Mater. Lett*., 67(2012), No. 1, p. 131.

[13] V.V. Srdić, R. Djenadić, M. Milanović, N. Pavlović, I. Stijepović, L.M. Nikolić, E. Moshopoulous, K. Giannakopoulos, J. Dusza, and K. Maca, Direct synthesis of nanocrystalline oxide powders by wet-chemical techniques, *Process. Appl. Ceram*., 4(2010), No. 3, p. 127.

[14] Y.M. Rangel-Hernandez, J.C. Rendón-Angeles, Z. Matamoros-Veloza, M.I. Pech-Canul, S. Diaz-de la Torre, and K. Yanagisawa, One-step synthesis of fine $SrTiO_3$ particles using $SrSO_4$ ore under alkaline hydrothermal conditions, *Chem. Eng. J*., 155(2009), No. 1-2, p. 483.

[15] Z.K. Zheng, B.B. Huang, X.Y. Qin, X.Y. Zhang, and Y. Dai, Facile synthesis of $SrTiO_3$ hollow microspheres built as assembly of nanocubes and their associated photocatalytic activity, *J. Colloid Interface Sci*., 358(2011), No. 1, p. 68.

[16] B.L. Gersten, Growth of multicomponent perovskite oxide crystals: synthesis conditions for the hyrothermal growth of ferroelectric powders, [in] K. Byrappa and T. Ohachi, *Crystal Growth Technology*, 2003, p. 299.

[17] R. Wongmaneerung, R. Yimnirun, and S. Ananta, Effect of vibro-milling time on phase formation and particle size of lead titanate nanopowders, *Mater. Lett*., 60(2006), No. 12, p. 1447.

[18] L.Q. Jing, Y.C. Qu, B.Q. Wang, S.D. Li, B.J. Jiang, L.B. Yang, W. Fu, H.G. Fu, and J.Z. Sun, Review of photoluminescence performance of nano-sized semiconductor materials and its relationships with photocatalytic activity, *Sol. Energy Mater. Sol. Cells*, 90(2006), No. 12, p. 1773.

[19] M.A. Behnajady, M.E. Alamdari, and N. Modirshahla, Investigation of the effect of heat treatment process on characteristics and photocatalytic activity of TiO_2-UV100 nanoparticles, *Environ. Prot. Eng*., 39(2013), No. 1, p. 33.

[20] L.F. da Silva, L.J.Q. Maia, M.I.B. Bernardi, J.A. Andrés, and V.R. Mastelaro, An improved method for preparation of $SrTiO_3$ nanoparticles, *Mater. Chem. Phys*., 125(2011), No. 1-2, p. 168.

[21] F.M. Pontes, E.R. Leite, E.J.H. Lee, E. Longo, and J.A. Varela, Preparation, microstructural and electrical characterization of $SrTiO_3$ thin films prepared by chemical route, *J. Eur. Ceram. Soc*., 21(2001), No. 3, p. 419.

[22] S.W. Liu, Z.L. Xiu, J.A. Liu, F.X. Xu, W.N. Yu, J.X. Yu, and G.J. Feng, Combustion synthesis and characterization of perovskite $SrTiO_3$ nanopowders, *J. Alloys Compd*., 457(2008), No. 1-2, p. L12.

[23] Y.T. Zheng, Z.L. Zhang, and Y.L. Mao, Photovoltaic response enhancement of $SrTiO_3/TiO_2$ composite, *J. Alloys Compd*., 554(2013), p. 204.

[24] A.F. Demirörs and A. Imhof, $BaTiO_3$, $SrTiO_3$, $CaTiO_3$, and $Ba_xSr_{1-x}TiO_3$ particles: a general approach for monodisperse colloidal perovskites, *Chem. Mater*., 21(2009), No. 13, p. 3002.